Raport Badawczy

Research Report

RB/69/2001

PI compensation of time delayed processes based on phase margin and crossover frequency

W. Krajewski, A. Lepschy, U. Viaro

Instytut Badań Systemowych
Polska Akademia Nauk

Systems Research Institute
Polish Academy of Sciences

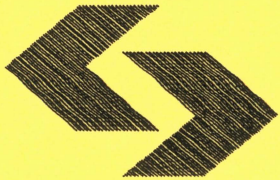

POLSKA AKADEMIA NAUK

Instytut Badań Systemowych

ul. Newelska 6

01-447 Warszawa

tel.: (+48) (22) 8373578

fax: (+48) (22) 8372772

Pracę zgłosił: prof. dr hab. inż. Krzysztof Kiwiel

Warszawa 2001

PI compensation of time delayed processes based on phase margin and crossover frequency ⋆

Wieslaw Krajewski [a], Antonio Lepschy [b], Umberto Viaro [c]

[a] *Systems Research Institute, Polisch Academy of Sciences, ul. Newelska 6, 01 447 Warsaw, Poland*

[b] *Department of Electronics and Informatics, University of Padova, via Gradenigo 6/A, 35131 Padova, Italy*

[c] *Department of Electrical, Managerial and Mechanical Engineering, University of Udine, via delle Scienze 208, 33100 Udine, Italy*

Abstract

Simple procedures and charts are suggested to design PI controllers for time delayed processes so as to meet specified phase margin and cross-over frequency. The compatibility of the specifications with system stability and their influence on system performance are investigated. It is shown how the procedures can be extended to the case in which the specifications are given in terms of gain and phase margins. Robustness issues are also considered.

Key words: PI controllers; First-order lag plus dead-time process models; Stability margins; Parameter-plane stability regions; Cross-over frequencies.

1 Introduction

1.1 Problem statement

Following the work of Ziegler and Nichols (Ziegler & Nichols, 1942) a variety of PID design methods have been suggested (Aström & Hägglund, 1995;

⋆ This paper was not presented at any IFAC meeting. Corresponding author A. Lepschy. Tel. +39(0)49 827 7612. Fax +39(0)49 827 7699.

Email addresses: krajewsk@ibspan.waw.pl (Wieslaw Krajewski), lepschy@dei.unipd.it (Antonio Lepschy), viaro@uniud.it (Umberto Viaro).

O'Dwyer, 2000a,b,c; Syder et al., 2000), which is not surprising in view of the very large number of industrial control systems including such kind of controllers (Yamamoto & Hashimoto, 1991; Aström & Hägglund, 1995).

Many processes can adequately be represented by a first-order lag plus delay, i.e., by a model for which efficient identification techniques have been developed O'Dwyer (2000d). In the following reference will be made to such a model. However, since it is necessarily only an approximation of the actual plant behaviour, robustness issues play a major role.

Traditionally, stability margins have been used as meaningful measures of robustness with respect to both system stability and performance, and PID design techniques have been developed to satisfy gain and phase margin specifications, possibly in conjunction with performance optimization criteria (Ho et al., 1995a,b, 1997, 1998, 1999, 2001). In particular, the equations expressing the magnitude and phase of the loop frequency response have been solved numerically for the cross-over frequencies and controller parameters, and the ISE for various combinations of stability margins have been computed to allow a tradeoff between these margins and performance (Ho et al., 1999).

In this paper a partially different path is followed. First, some remarks on the choice of the design specification are made to justify the preference for those based on the phase margin m_ϕ and gain cross-over frequency ω_A, even if the suggested procedure can be adapted to the case in which the specifications are given in terms of phase and gain margins. By limiting attention to PI controllers, the specifications are immediately translated into linear interpolation conditions that allow us to easily determine the controller parameters from those of the process. The evaluation of the compatibility of mf and wA with the system stability, their influence on its performance, and the choice of the design parameters are facilitated by suitable charts showing the regions of the controller parameter plane corresponding to given ranges of stability margins and cross-over frequencies. The use of these charts is illustrated with the aid of examples. Charts of the same kind are suggested for the case in which the specifications are in terms of phase and gain margins.

1.2 Remarks on the specifications

Specifications should concern the following aspects of the system behaviour:

- (internal) stability and stability robustness, usually evaluated in terms of phase margin m_ϕ and gain margin m_g;
- steady-state precision, characterized by means of loop tipe and of the steady-state error ess in the response to the relevant canonical input (unit step ant its integrals), which depends on the Bode gain of the loop function;

- dynamic precision, related to the overshoot m_p of the step response, or to the resonance peak M_r of the frequency response, which are in turn strictly connected with the phase margin;
- promptness of the response, characterized by both the settling time and the rise time, the latter being related to the pass-band B of the frequency response and, therefore, to the gain cross-over frequency ω_A.

The assumptions on the process dynamics, approximated by means of a first order model plus a dead time, and on the PI structure of the controller, ensure that the loop is of type one (no steady-state error in the step response). Since, usually, the steady-state error in the response to a ramp input is not so important, the Bode gain of the loop function and, consequently, the coefficient K_I of the controller integral action will be determined with reference to other aspects of the system behaviour. Also, the magnitude of the open-loop frequency response turns out to be monotonically decreasing, so that, in general, a rather large phase margin implies an acceptable gain margin too. In conclusion, to characterize stability and dynamic precision, reference will be made to the phase margin and, to characterize promptness, to the gain cross-over frequency. In this way, the number of specifications matches that of the controller parameters. Clearly, the choice of these specifications may require successive adjustments of the controller parameters so as to obtain acceptable values of the overshoot m_p (not rigidly related to m_ϕ), of the rise and settling times (not rigidly related to ω_A) and of the gain margin (accounting for the robustness with respect to gain variations).

1.3 Model normalization

In the following, reference will be made to processes that can adequately be modelled by a transfer function of the form:

$$\hat{P}(\hat{s}) = K\frac{e^{-L\hat{s}}}{1+T\hat{s}},\ K,T,L>0 \tag{1}$$

where the independent variable has been denoted by $\hat{s}$ because the symbol s will be used to indicate a normalized variable.

The transfer function of the adopted PI controller will be denoted by:

$$\hat{C}(\hat{s}) = K_P + \frac{K_I}{\hat{s}} = \frac{K_I}{\hat{s}}(1+T_I\hat{s}) = K_P(1+\frac{1}{T_I\hat{s}}) \tag{2}$$

with

$$T_I = \frac{K_P}{K_I}. \tag{3}$$

Therefore, the open-loop transfer function becomes:

$$\hat{G}(\hat{s}) = \frac{K(K_I + K_P\hat{s})}{\hat{s}} \frac{e^{-L\hat{s}}}{1 + T\hat{s}}. \tag{4}$$

For the reasons explained in Section 1.2, we initially consider specifications in terms of phase margin m_ϕ and gain cross-over frequency $\hat{\omega}_A$.

For normalization purposes, the independent variable will be changed to:

$$s := T\hat{s} \tag{5}$$

so that (4) becomes:

$$G(s) := \hat{G}(\frac{s}{T}) = \frac{(a + b\,s)}{s} \frac{e^{-\tau s}}{1 + s}. \tag{6}$$

where:

$$a := KK_IT, \tag{7a}$$

$$b := KK_P, \tag{7b}$$

$$\tau := \frac{L}{T}. \tag{7c}$$

Accordingly, the specification on $\hat{\omega}_A$ is translated into a constraint on the normalized cross-over frequency:

$$\omega_A := T\hat{\omega}_A, \tag{8}$$

whereas the specification on m_ϕ is not affected by (5).

2 Interpolation conditions

It is easy to relate the values of parameters a and b to the values of ω_A and m_ϕ, given the value of τ (which is the unique parameter characterizing the

process in the normalized transfer function function (6)). Once a and b have been determined, the controller parameters K_P and K_I, or K_P and T_I, can be obtained from (7a), (7b) and (7c).

Necessary conditions for $G(j\omega)$ to exhibit phase $m_\phi - \pi$ and unit magnitude at ω_A follow immediately from the interpolation condition:

$$G(j\omega_A) = \cos(m_\phi - \pi) + j\sin(m_\phi - \pi) = -\cos m_\phi - j\sin m_\phi. \tag{9}$$

Multiplying (9) by the denominator of $G(j\omega_A)$, for ω_A real and strictly positive we get:

$$a\cos(\tau\omega_A) + b\omega_A\sin(\tau\omega_A) = \omega_A^2\cos m_\phi + \omega_A\sin m_\phi, \tag{10a}$$

$$-a\sin(\tau\omega_A) + b\omega_A\cos(\tau\omega_A) = -\omega_A\cos m_\phi + \omega_A^2\sin m_\phi, \tag{10b}$$

Clearly, conditions (10a), (10b) are not sufficients to achieve the desired stability margin m_ϕ because, even if the Nyquist diagram of $G(j\omega)$ passes through point $e^{j(m_\phi-\pi)}$, it could encircle point $-1+j0$ (see later).

A useful feature of eqs (10a), (10b) is their linearity with respect to a and b, which allows us to easily find their unique solution:

$$a = \omega_A[\sin(\tau\omega_A + m_\phi) + \omega_A\cos(\tau\omega_A + m_\phi)], \tag{11a}$$

$$b = \omega_A\sin(\tau\omega_A + m_\phi) - \cos(\tau\omega_A + m_\phi). \tag{11b}$$

In the following sections, these equtions will be exploited to check the compatibility between the considered specifications, to design the controller and, also, to evaluate the system robustness. However, a stability analysis must preliminarily be performed.

3 Stability analysis

The Nyquist diagram of the type-one loop function $G(j\omega)$ for $\omega \longrightarrow 0_+$ tends to a vertical asymptote whose abscissa turns out to be:

$$r := \lim_{\omega\to 0} Re[G(j\omega)] = b - (1+\tau)a. \tag{12}$$

Moreover we have:

$$sgn\{\lim_{\omega\to 0_+} Im[G(j\omega)]\} = -sgn\, a. \tag{13}$$

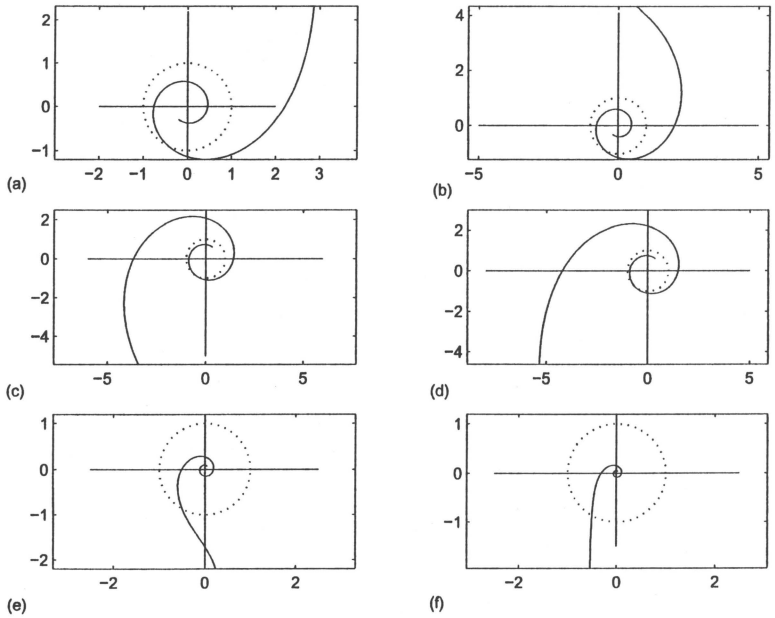

Fig. 1. Typical Nyquist diagrams for (6).

It follows that the initial arc (ω small) of the (positive) Nyquist diagram belongs to:

(i) the first quadrant for $a < 0$, $b > (1 + \tau)a$;
(ii) the second quadrant for $a < 0$, $b < (1 + \tau)a$;
(iii) the third quadrant for $a > 0$, $b < (1 + \tau)a$;
(iv) the fourth quadrant for $a > 0$, $b > (1 + \tau)a$.

The first two cases, exemplified in Fig. 1a and Fig. 1b, correspond to unstable behaviour as immeditely shown by the Nyquist criterion. The last two cases ($a > 0$) may correspond to either unstable behaviour, as in Fig. 1c and Fig. 1d, or stable behaviour, as in Fig. 1e and Fig. 1f. Therefore the stability region in the (a, b)-plane may only belong to the right half-plane ($a > 0$). By taking into account that $|G(j\omega)|$ decreases monotonically as ω increases (which would not be true in the case of the PID controllers), the positive Nyquist diagram intersects the unit circle at one point only. For every value of τ, the stability boundary is formed by a segment of the b-axis ($a = 0$) and by the curve of

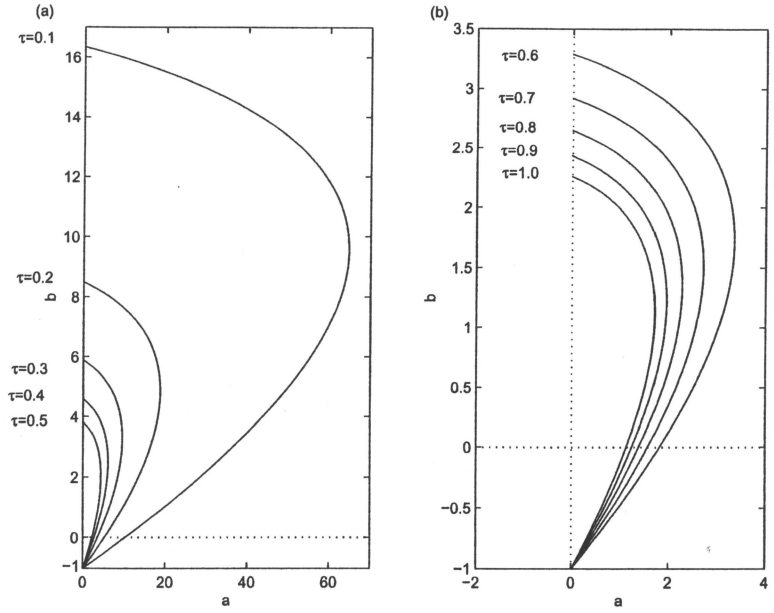

Fig. 2. Stability regions of the (a, b)-plane: (a) $\tau = 0.1 \div 0.5$; (b) $\tau = 0.6 \div 1.0$

the (a, b)-plane characterized by:

$$\arg[G(j\omega_A)] = -\pi \tag{14}$$

along which $m_\phi = 0$. (Note that, if $\arg[G(j\omega_A)] = -(2k+1)\pi$, $k \in Z_+$, the system would not be stable because the Nyquist diagram would encircle the critical point).

The curves of the (a, b)-plane corresponding to m_ϕ constant, $m_\phi > 0$, develop inside the above mentioned stability boundary and their extremes lay on the b-axis. It is not easy to find their analytic expression either in the explicit form $b = f(a)$ or in the implicit form $g(a, b) = 0$. Nevertheless, it can be obtained from $(11a)$, $(11b)$, e.g., using MATLAB.

The stability boundaries for various values of τ are depicted in Fig. 2, whereas the curves corresponding to a set of values of m_ϕ for the same value of τ are given in Fig. 3.

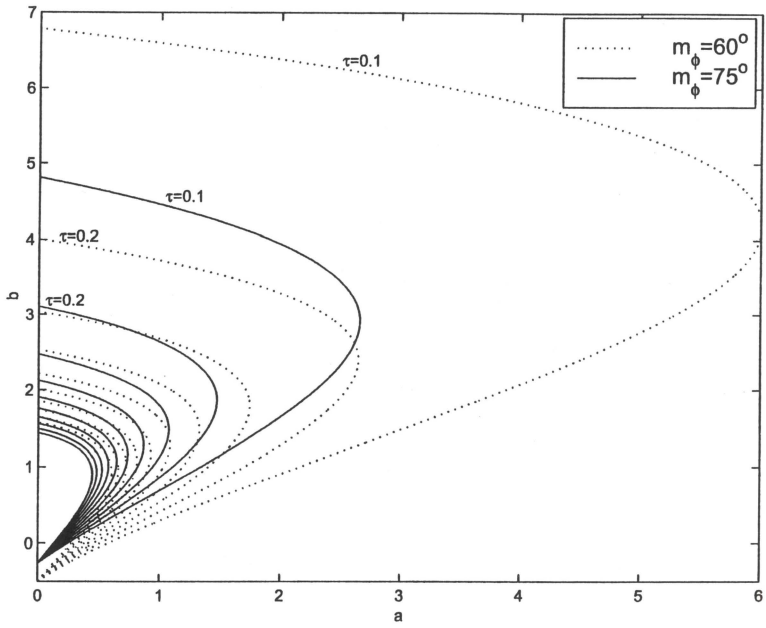

Fig. 3. Curves $m_\phi = const$ in the (a, b)-plane $\tau = 0.5$

4 Gain cross-over frequencies

The analytic expression of the curves on the (a, b)-plane corresponding to $\omega_A = const$ can immediately be determined from the condition $|G(j\omega_A)| = 1$. In fact, taking account of (6) and considering square magnitudes, we get:

$$\frac{a^2 + b^2\omega_A^2}{\omega_A^2(1+\omega_A^2)} = 1 \tag{15}$$

and then:

$$a^2 + \omega_A^2 b^2 - \omega_A^2 - \omega_A^4 = 0 \tag{16}$$

which represents an ellipse centered at $(a = 0, b = 0)$ whose axes belong to the straight lines $a = 0$ and $b = 0$. These ellipses intersect the vertical axis at

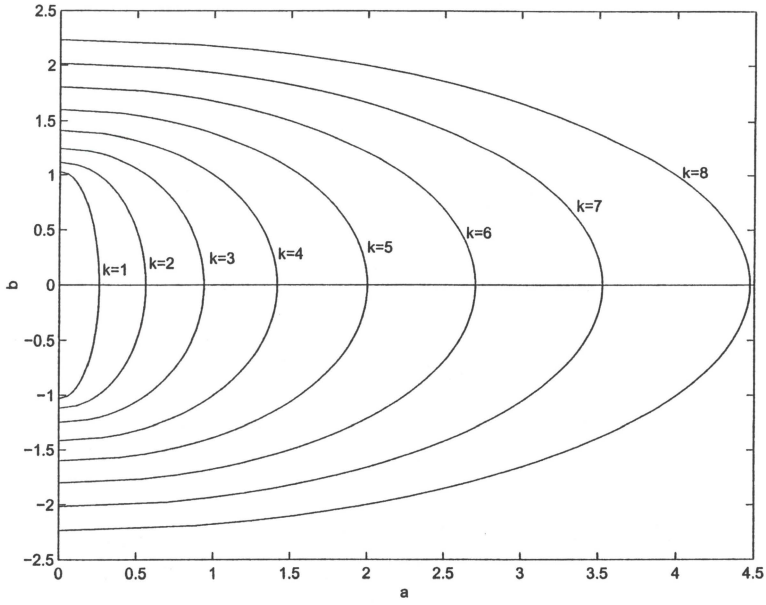

Fig. 4. Arcs of the curves $\omega_A = 0.25k$, $k = 1 \div 8$.

$a = 0$ and

$$b = \pm\sqrt{1+\omega_A^2}, \tag{17}$$

whereas they intersect the horizontal axis at $b = 0$ and

$$a = \pm\omega_A\sqrt{1+\omega_A^2}. \tag{18}$$

In particular, for $\omega_A = 1$ the ellipse becomes a circle of radius $\sqrt{2}$; for $\omega_A < 1$ the horizontal axis is smaller than vertical one, and vice versa for $\omega_A > 1$. It is interesting to observe that the ellipse corresponding to ω_A, $\forall\omega_A$, intersects the line $b = a$ at $b = a = \omega_A$.

Note, also, that ellipses (16) are independent of τ (whereas the curves $m_\phi = const$ depend on it) and that only their right halves may belong to the stability region. Fig. 4 shows arcs of the ellipses corresponding to different values of ω_A in the region of interest.

5 Specification compatibility

According to the considerations of Section 1, let us assume that the specifications are:

$$m_\phi \geq m_\phi^\star, \tag{19}$$

$$\omega_A = \omega_A^\star. \tag{20}$$

Given the process to be controlled, i.e., given τ, reference will be made to the ellipse $\omega_A = \omega_A^\star$ and to the curve $m_\phi = m_\phi^\star$ corresponding to such τ. The above specifications are compatible with each other iff an arc of the ellipse $\omega_A = \omega_A^\star$ belong to the region between the curve $m_\phi = m_\phi^\star$ and the vertical axis. For instance, for $\tau = 0.5$ the condition $\omega_A = 2$ is not compatible with $m_\phi \geq 75°$, whereas it is compatible with $m_\phi \geq 45°$: in fact, as shown in Fig. 5, the curve $\omega_A = 2$ is external to the curve $m_\phi \geq 75°$, whereas it intersects the curve $m_\phi = 45°$ at point P_1 so that the points of arc P_1P_2 exibit a phase margin greater than 45° (precisely, it ranges from 45° to almost 60°).

On the other hand, it is easy to find the highest value ω_A^u of ω_A compatible with a given m_ϕ because it corresponds to the value b_u of b characterizing the upper intersection of the curve for relevant phase margin with the vertical axis, where the cross-over frequency takes the value (cf. (17)):

$$\omega_A^u = \sqrt{b_u^2 - 1}. \tag{21}$$

In this regard, it may be useful to exploit the fact that for $\tau \in [0.1, 1]$ the dependence of b_u on τ is very well approximated by the hyperbola:

$$b_u = \mu \frac{1}{\tau} + \nu \tag{22}$$

where μ and ν are constants dependent on m_ϕ. Tab. 1 gives the mean square values μ and ν for various values of m_ϕ. Once b_u has been estimated, ω_A^u can be computed using (21).

Table 1. Coefficients of (22)

m_ϕ	30°	45°	60°	75°	90°	120°
μ	1.0562	0.8142	0.5799	0.3760	0.2173	0.0562
ν	0.8427	0.9017	1.0414	1.1322	1.1820	1.1338

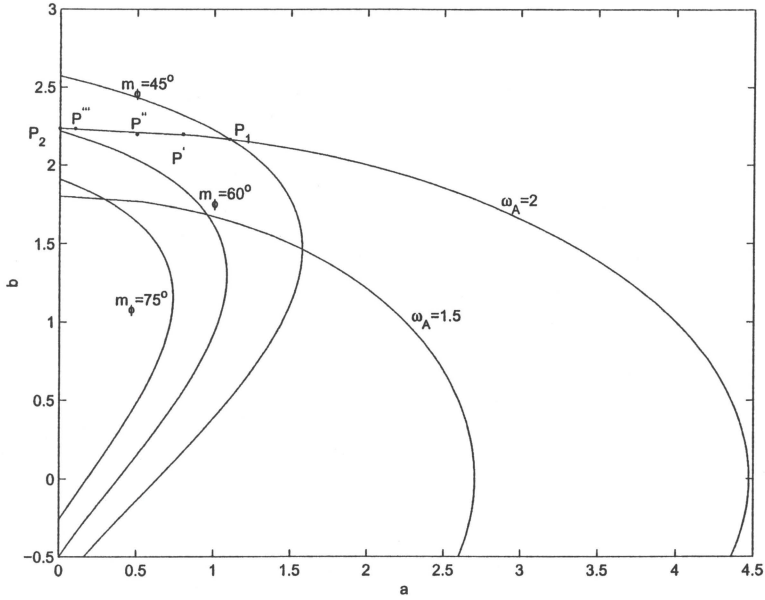

Fig. 5. Compatibility of the conditions $\omega_A^\star = 2$ and $\omega_A^\star = 1.5$ with $m_\phi \geq 75°$, $m_\phi \geq 60°$ and $m_\phi \geq 45°$ for $\tau = 0.5$.

6 Design charts and robustness analysis

To facilitate the design of procedure, it is convenient to avail ourselves of charts depicting a number of loci $m_\phi = const$ and $\omega_A = const$ in the region of interest of the (a, b)-plane for different values of τ. Charts of this kind are shown in Fig. 6.

With reference to specifications (19) and (20) and to the value of τ characterizing the normalized process, the design procedure consists of the following steps:

(i) choose the chart corresponding to the value of $\tau = \frac{L}{T}$ closest to the actual normalized delay;
(ii) if the specifications are not compatible, either modify the normalized gain cross-over frequency $\omega_A^\star$ or resort to a more complicated controller (e.g., a PID controller);
(iii) determine (if necessary, by interpolation) the coordinates (a, b) of a point

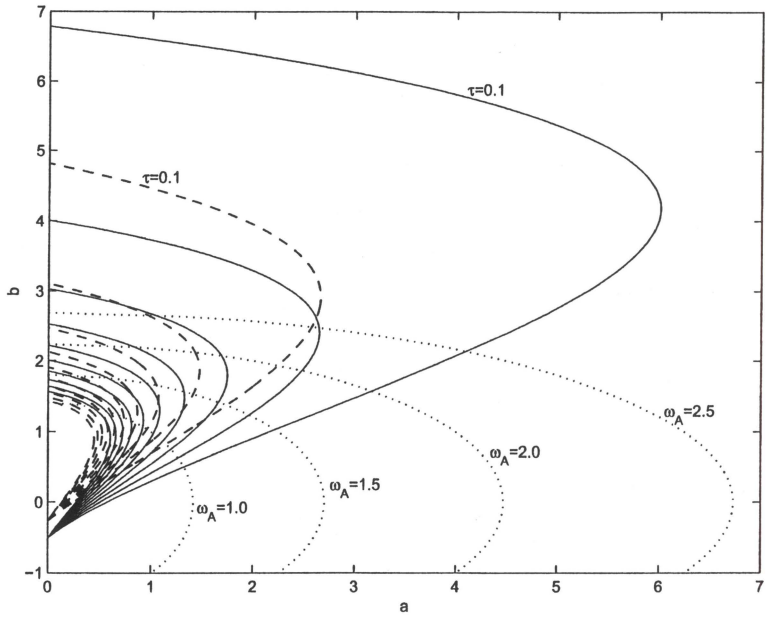

Fig. 6. Loci $m_\phi = 60°$ (solid lines), $m_\phi = 75°$ (dashed lines) and $\omega_A = const$ (dotted lines) in the (a, b)-plane for $\tau = 0.1k$, $k = 1 \div 10$.

P on the curve $\omega_A = \omega_A^\star$ included between its intersections with the curve $m_\phi = m_\phi^\star$ and the vertical axis, like points P_1 and P_2 in Fig. 5 (concerning the choice of P see later);

(iv) using relations $(7a)$, $(7b)$ and $(7c)$ compute K_P and K_I or T_I as:

$$K_P = \frac{b}{K}, \qquad K_I = \frac{a}{KT} \qquad \text{or} \qquad T_I = \frac{bT}{a}. \tag{23}$$

The above charts can also be used to evaluate the effects on m_ϕ and $\hat{\omega}_A$ of a change in the process parameters.

To this purpose, let us denote by K_P and K_I the values of the controller parameters ensuring the satisfaction of the specifications $m_\phi = \bar{m}_\phi \leq m_\phi^\star$ and $\hat{\omega}_A = \hat{\omega}_A^\star$ when the process parameters are K, L and T, and denote K', L' and T' their modified values. By keeping the controller unchanged, the new process parameters lead to the following values for the parameters of the normalized

loop transfer function (cf. (7*a*), (7*b*) and (7*c*)):

$$a' = K' K_I T', \qquad b' = K' K_P, \qquad \tau' = \frac{L'}{T'}. \tag{24}$$

Using the chart for τ', the new phase margin m'_ϕ and normalized cross-over frequency ω'_A corresponding to (a', b') can be evaluated, from which the new actual cross-over frequency $\hat{\omega}'_A = \frac{\omega'_A}{T'}$ is immediately obtained.

A reasonable measure of the effects of the considered process modification is provided by the deviation Δm_ϕ and $\Delta\hat{\omega}_A$ of the new values m'_ϕ and $\hat{\omega}'_A$ from the old values $\bar{m}_\phi$ and $\hat{\omega}^*_A$ of the phase margin and cross-over requency corresponding to the old pair (a, b), i.e.:

$$\Delta m_\phi := m'_\phi - \bar{m}'_\phi, \tag{25}$$

$$\Delta\hat{\omega}_A := \hat{\omega}'_A - \hat{\omega}^*_A. \tag{26}$$

In practice, it will be only possible to predict the ranges $[K_m, K_M]$, $[L_m, L_M]$, $[T_m, T_M]$ over which the process parameters K, L, T, respectively, can vary. These intervals define a parallelepiped of the original process parameter space that is mapped via relations (7*a*), (7*b*), (7*c*), with K_P and K_I constant, into a solid of the (a, b, τ) space characterized by $2^3 = 8$ vertices and 12 edges. The determination of the worst case, in terms of both Δm_ϕ and $\Delta\hat{\omega}_A$, is facilitated by the use of programs, e.g., in MATLAB, for representing the cross sections of this solid on the charts for a suitable number of τ values in the interval of interest, i.e., $\tau \in [\frac{L_m}{T_M}, \frac{L_M}{T_m}]$. As far as m_ϕ is concerned, the worst case usually corresponds to the vertex $[K_M, L_M, T_m]$.

7 Gain margin

The Nyquist diagram of the loop function (6) crosses the negative real semi-axis an infinite number of times. The value of ω_B of the frequency ω corresponding to the first intersection is the so-called phase cross-over frequency. Denoting by g the absolute value of (6) at this point, we have:

$$G(j\omega_B) = -g. \tag{27}$$

As is known, the gain margin m_g can be defined in different ways, e.g., $m_g = 1 - g$ or $m_g = \frac{1}{g}$ or, especially with reference to Bode diagrams, $m_g = \log\frac{1}{g} = -\log g$. To simplify the analysis, in the following, we directly

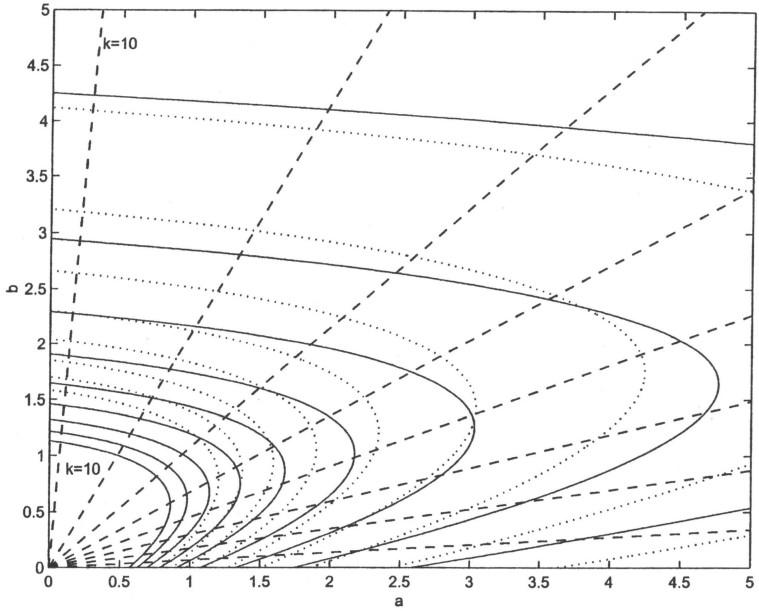

Fig. 7. Curves $g = 0.5$ (solid lines), $g = 0.7$ (dotted lines) and lines $\omega_B = 2$ (dashed lines) for $\tau = 0.1k$, $k = 1 \div 10$, inside the stability region of the (a, b)-plane.

refer to g, from which it is immediate to obtain the gain margin, whatever definition is adopted.

Multiplying both sides of (27) by the denominator of $G(j\omega_B)$ and equating real and imaginary parts, we get:

$$a = g\,\omega_B[\sin(\tau\omega_B) + \omega_B \cos(\tau\omega_B)], \tag{28a}$$

$$b = g[\omega_B \sin(\tau\omega_B) - \cos(\tau\omega_B)]. \tag{28b}$$

Given τ, for any value of g eqns. (28a) and (28b) define a curve in the (a, b)-plane with current copordinate ω_B. Of course, the curve for $g = 1$ coincides with the curve characterized by $m_\phi = 0$ of the family previously considered, and forms the boundary of the stability region together with the relevant segment of the b-axis. Inside the stability region, the curves $g = \text{const}$ $(0 < g < 1)$ have the shape shown in Fig. 7. Their form is roughly similar to that of the curves for $m_\phi = \text{const}$ (cf. Fig. 6). However, the two intersections of

every g = const with the vertical axis include point $(0,0)$, whereas the two intersections of every curve m_ϕ = const include point $(0,1)$.

Concerning the curves ω_B = const (which determine the parametrization of those for g = const), their analytic expression, easily obtained from (28a) and (28b, is simply:

$$b = pa \tag{29}$$

with coefficient p given by:

$$p = \frac{\omega_B \sin(\tau\omega_B) - \cos(\tau\omega_B)}{\omega_B[\sin(\tau\omega_B) + \omega_B \cos(\tau\omega_B)]}, \tag{30}$$

which corresponds to a straight line through the origin whose slope does not depend on g but depends on τ. These lines too, are represented in Fig. 7.

The charts in Fig. 7 allow us to find the gain margin (and the related phase cross-over frequency $\omega_B > \omega_A$) associated with a pair (a,b) determined according to the design procedure of Section 5, i.e., satisfying the specifications on m_ϕ and ω_A, and can thus be used to discriminate the points of the "admissible" arc of the parameter plane (like arc P_1P_2 of Fig. 5): note in this regard, that a not too small value of g is often preferable (see later).

Clearly, if the design is based on m_ϕ and m_g, instead of m_ϕ and ω_A, it is useful to avail ourselves of charts depicting, for every τ, the curves $m_\phi = const$ inside the stability region. In this case, by denoting with $m_\phi^\star$ and $g^\star$ the specified lower bound on m_ϕ and upper bound on g, the specifications are compatible iff curve $m_\phi = m_\phi^\star$ crosses curve $g = g^\star$ on the chart for the relevant value of τ, and the acceptable values of the normalized controller parameters will correspond to the points in the intersection of the regions where $m_\phi \geq m_\phi^\star$ and $g \leq g^\star$. The procedure is exemplified in Fig. 8 with reference to $\tau = 0.5$, $m_\phi^\star = 60^o$, and $g^\star = 0.3$: curves $m_\phi = 60^o$ and $g = 0.3$ intersect at $(1, 0.91\bar{6})$ for $\omega_A = 0.96$ and at $(0.221, -0.200)$ for $\omega_A = 0.21$. The Nyquist diagrams of the loop functions corresponding to these two points practically coincide, except for their graduation in ω, along the arc between the intersection with the real axis, and slightly differ outside this arc. Correspondingly, the overshoots of the step responses of the two feedback systems are about the same, whereas the ratio between their rise times is almost the reciprocal of the ratio between the related gain cross-over frequencies.

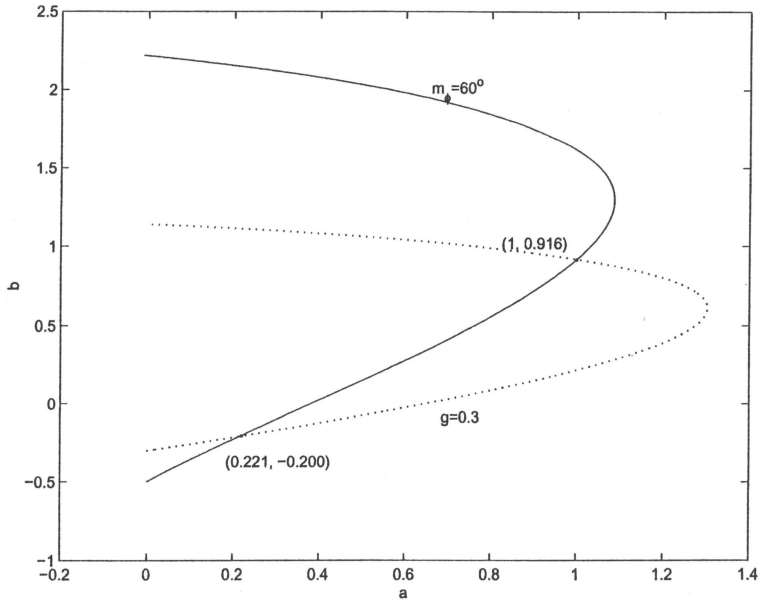

Fig. 8. Regions where $m_\phi \geq 60^o$ and $g \leq 0.3$ for $\tau = 0.5$.

8 Choice of point (a, b) in the admissible region

If the specifications are compatible, they can be satisfied in different ways. The following considerations help us identify the solutions that are most satisfactory (for the specific problem at hand).

As already said, if the specifications are given in terms of gain cross-over frequency and phase margin, i.e., in the form $\omega = \omega_A^\star$ and $m_\phi \geq m_\phi^\star$, the admissible region of the (a, b)-plane reduces to the arc of the ellipse $\omega_A = \omega_A^\star$ between its intersections with the curve $m_\phi = m_\phi^\star$ and the b-axis, like arc P_1P_2 of Fig. 5 which refers to the case of $\tau = 0.5$, $\omega_A^\star = 2$ and $m_\phi^\star = 45^o$. It is instructive to examine the step response of the feedback control system corresponding to different points of arc P_1P_2. To this purpose, Fig. 9 shows the responses for:

(i) point $P_1 = (1.1023, 2.1671)$, where $m_\phi = 45^o$;
(ii) point $P' = (0.8, 2.2)$, where $m_\phi \simeq 49^o$;
(iii) point $P'' = (0.5, 2.\bar{2})$, where $m_\phi \simeq 53^o$;

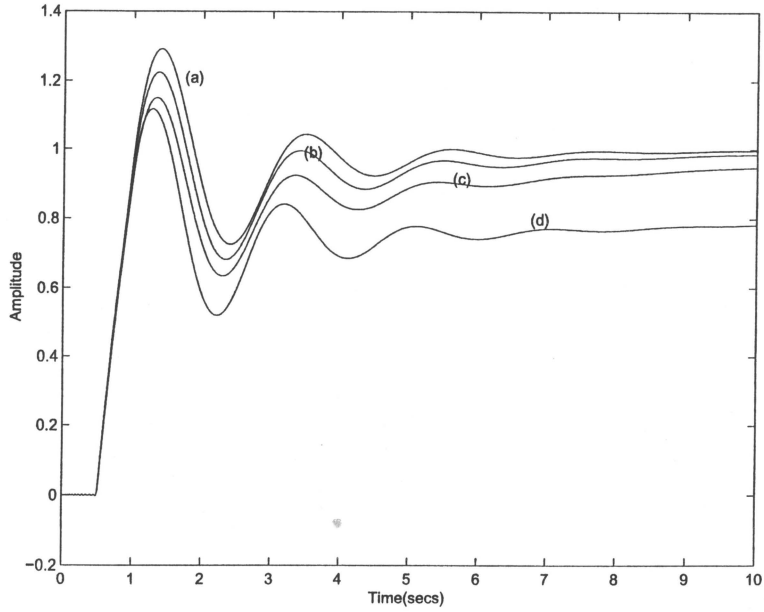

Fig. 9. Step responses of the feedback control system for $\tau = 0.5$, $\omega_A = \omega_A^\star = 2$ and $m_\phi \geq m_\phi^\star = 45^o$: (a) $a = 1.1023$, $b = 2.1671$ ($m_\phi = 45^o$); (b) $a = 0.8$, $b = 2.2$ ($m_\phi \approx 49^o$); (c) $a = 0.5$, $b = 2.2$ ($m_\phi \approx 53^o$); (d) $a = 0.1$, $b = 2.2355$ ($m_\phi \approx 58^o$).

(iv) point $P''' = (0.1, 2.2355)$, very close to P_2, where $m_\phi \simeq 58^o$.

For $t > \tau$, all responses are well approximated by the step response of a third-order system with two complex poles. On passing from P_1 to P_2, the importance of the above slow aperiodic mode increases. As a result, the time to reach half the final value and the rise time remain (practically) unchanged, whereas the overshoot, strictly related to the phase margin, decreases and the settling time increases.

Similar conclusions can be drawn with reference to the step responses represented in Fig. 10, which correspond to the intersections of the ellipse $\omega_A = 1.5$ with the curves $m_\phi = 45^o$, $m_\phi = 60^o$ and $m_\phi = 75^o$, also shown in Fig. 5. The last two intersections, like the points on the arc P_1P_2 considered in Fig. 9, lie above the line $b = a$, along which, as already observed in Section 3, the gain cross-over frequency is $\omega_A = a = b$, the first intersection, insted, is below this line, but quite close to it. Now, for $a = b$ the the zero introduced by

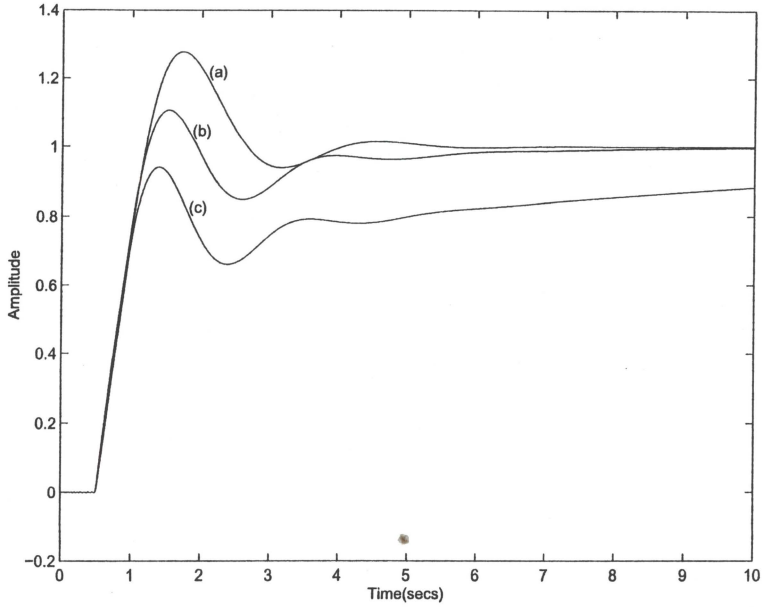

Fig. 10. Step responses for $\tau = 0.5$, $\omega_A = 1.5$ and: (a) $m_\phi = 45^o$ ($a = 1.5786$, $b = 1.4637$); (b) $m_\phi \approx 60^o$ ($a = 0.9566$, $b = 1.686$); (c) $m_\phi \approx 75^o$ ($a = 0.2842$, $b = 1.7859$).

the controller cancels the pole of the process at -1 and the feedback system exhibits only two dominant poles, which can easily be explained with the aid of root locus considerations (its part closest to the origin contains arcs of two branches only). For this reason, for $t > \tau$ the step response corresponding to $\omega_A = 1.5$ and $m_\phi = 45^o$ (curve (a) of Fig. 10) is very similar to that of a second-order system, whereas the other responses are characterized by three dominant poles (the poles closest to the origin) and, therefore, contain an additional (aperiodic) mode.

Concerning the choice of a point in the admissible region when the specifications are in terms of phase and gain margins, let us consider again the example illustrated in Fig. 8 The point $(1, 0.91\bar{6})$ at the intersection of the curves $m_\phi = m_\phi^\star = 60^o$ and $g = g^\star = 0.3$ is very near the straight line $b = a$. The step response of the related feedback control system is represented in Fig. 11 together with the responses for $a = b = 0.75$ (where the settling time is almost minimal) and $a = b = 0.5$ corresponding to points inside the admisible

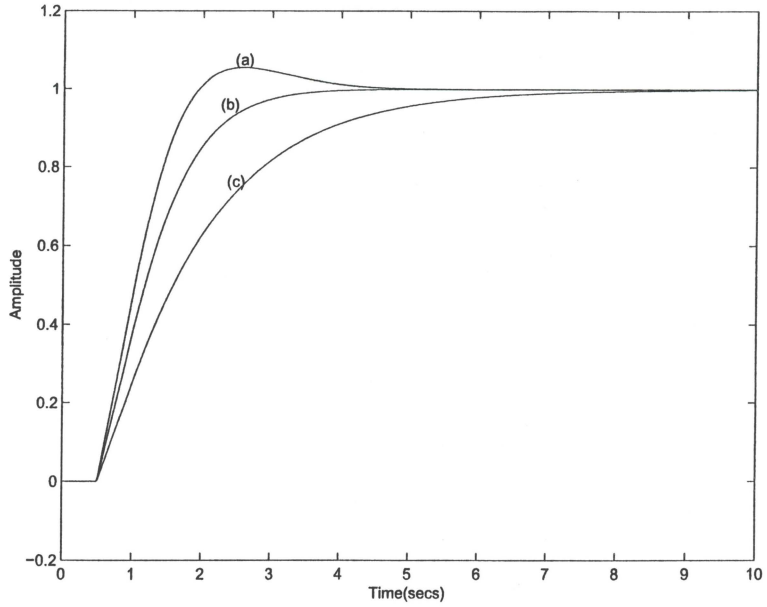

Fig. 11. Step responses for $\tau = 0.5$ corresponding to points on, or close to, the line $b = a$: (a) $a = 1.0$, $b = 0.916$ ($m_\phi = 60^o$, $g = 0.3$, $\omega_A = 0.96$); (b) $a = b = \omega_A = 0.75$ ($m_\phi = 68.5^o$, $g = 0.24$); (c) $a = b = \omega_A = 0.5$ ($m_\phi = 75.7^o$, $g = 0.16$).

region. For the reasons previously explained, all these responses are very similar to responses of a second-order system (for $t > \tau$). As the considered point approaches the origin along the above-mentioned line, m_ϕ increases (from 60^o to 75.7^o) and ω_A decreases (from 0.96 to 0.5). Correspondingly, the responses become monotonically increasing with longer rise times.

If, instead, the (a, b)-point approaches the b-axis along the horizontal line $b = 0.91\bar{6}$), the step responses change as shown in Fig. 12: the importance of the additional (aperiodic) dominant mode increases and the settling time becomes longer.

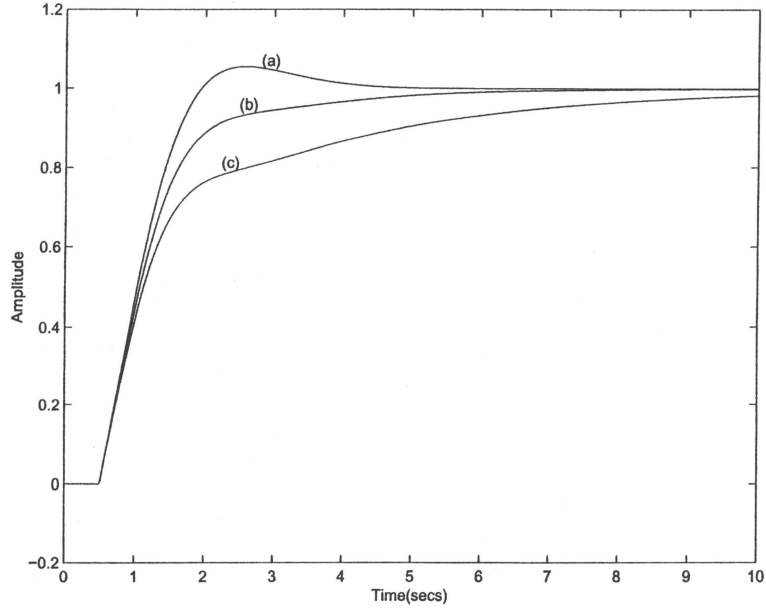

Fig. 12. Step responses for $\tau = 0.5$ corresponding to points on the horizontal line $b = 0.916$: (a) $a = 1.0$ ($m_\phi = 60^o$, $g = 0.3$, $\omega_A = 0.96$); (b) $a = 0.75$ ($m_\phi = 72.2^o$, $g = 0.28$, $\omega_A = 0.82$); (c) $a = 0.5$ ($m_\phi = 88.3^o$, $g = 0.26$ $\omega_A = 0.65$).

9 Conclusions

Formulae and charts have been provided that allow us to check the compatibility of the specifications and facilitate the design of PI controllers for time delayed processes. Precisely, with a suitable normalization the plant is characterized by the ratio τ between the actual dead time L and the time constant T and the controller by the coefficients $a = K_I KT$ and $b = K_P K$, the specifications concern the phase margin m_ϕ and the cross-over frequency ω_A, and the charts show for any τ the curves $m_\phi = const$ and $\omega_A = const$ in the (a, b)-plane. The compatibility between the considered specifications corresponds to the intersection of the related loci. Since a specification is expressed as an inequality, different solutions are admissible. The paper suggests criteria for their selection by taking into account robustness issues too. Finally, the loci of constant gain margin are considered, which can be employed: (i) to check the gain margin corresponding to the adopted design parameters, or (ii) to deter-

mine such parameters so as to meet specifications concerning both stability margins (and then check the cross-over frequency).

References

Ziegler, J.G. & Nichols, N.B. (1942). Optimum settings for automatic controllers. *Transactions of the ASME*, 64, 759-768.

Aström, K.J., & Hägglund, T. (1995). PID controllers: Theory, design, and tuning. *Instrument Society of America.*

Ho, W.K., Hang, C.C., & Zhou, J.H. (1995a). Performance and gain and phase margins of well-known PI tuning formulas. *IEEE Transactions on Control Systems Technology*, 3(2), 245-248.

Ho, W.K., Hang, C.C., & Cao, L.S. (1995b). Tuning of PID controllers based on gain and phase margin specifications. *Automatica*, 31(3), 497-502.

Ho, W.K., Gan, O.P., Tay, E.B., & Ang, E.L. (1996). Performance and gain and phase margins of well-known PID tuning formulas. *IEEE Transactions on Control Systems Technology*, 4(4), 473-477.

Ho, W.K., Hang, C.C., & Zhou, J.H.(1997). Self-tuning PID control of a plant with under-damped response with specifications on gain and phase margins. *IEEE Transactions on Control Systems Technology*, 5(4), 446-452.

Ho, W.K., Lim, K.W., & Xu, W. (1998). Optimal gain and phase margin tuning for PID controllers. *Automatica*, 34(8), 1009-1014.

Ho, W.K., Lim, K.W., Hang, C.C., & Ni, L.Y. (1999). Getting more phase margin and performance out of PID controllers. *Automatica*, 35, 1579-1585.

Ho, W.K., Lee, T.H., Han, H.P., & Hong, Y. (2001). Self-tuning IMC-PID control with interval gain and phase margins assignment. *IEEE Transactions on Control Systems Technology*, (9)3,535-541.

O'Dwyer, A. (2000a). A summary of PI and PID controller tuning rules for processes with time delay. Part 1: PI controller tuning rules. *Proceedings of PID'00: IFAC workshop on digital control,* Terrassa, Spain (pp. 175-180) (published in Digital control: Past, present and future of PID control, Pergamon Press, ISBN: 0-08-043624-2).

O'Dwyer, A. (2000b). A summary of PI and PID controller tuning rules for processes with time delay. Part 2: PID controller tuning rules. Proceedings of PID'00: *IFAC workshop on digital control,* Terrassa, Spain (pp. 242-247) (published in Digital control: Past, present and future of PID control, Pergamon Press, ISBN: 0-08-043624-2).

O'Dwyer, A. (2000c). PID compensation of time delayed processes: a survey. *Proceedings of the Irish Signals and Systems Conference*, Dublin, Ireland (pp. 5-12).

O'Dwyer, A. (2000d). Time delayed process model parameter estimation: A classification of techniques. *Proceedings of the international conference on control 2000*, Cambridge, England.

Silva, G.J., Datta, A., & Bhattacharyya, S.P. (2001). PI stabilization of first-order systems with time delay. *Automatica, scheduled for the December*, 2001, issue (37:12), paper no. 99509.

Syder, J., Heeg, T., & O'Dwyer, A. (2000). Dead-time compensators: performance and robustness issues. *Proceedings of process control and instrumentation 2000*, Glasgow.

Vrancic, D., Peng, W., & Strmcnik, S. (1999). A new PID controller tuning method based on multiple integrations. *Control Engineering Practice*, 7, 623-633.

Vrancic, D., Strmsnik, S., & Juricic, D. (2001). A magnitude optimum multiple integration tuning method for filtered PID controller. *Automatica*, 37, 1473-1479.

Yamamoto, S., & Hashimoto,I. (1991). Present status and future needs: The view from Japanese industry. Chemical Process Control - CPCIV: *Proceedings of the fourt international conference on chemical process control.* In Y. Arkun, Y., & W. H. Fay, New York: AIChE.